

# Examination of Dynamic Facilitation in Molecular Dynamics Simulations of Glass-Forming Liquids<sup>†</sup>

Magnus N. J. Bergroth,<sup>‡</sup> Michael Vogel,<sup>‡,||</sup> and Sharon C. Glotzer<sup>\*,‡,§</sup>

Departments of Chemical Engineering and Materials Science & Engineering, University of Michigan, Ann Arbor, Michigan 48109-2136

Received: November 14, 2004; In Final Form: March 1, 2005

Using data from molecular dynamics computer simulations of the one-component Dzugutov liquid and of BKS silica in metastable equilibrium supercooled states, we examine ideas introduced by Garrahan and Chandler (GC) in their dynamic facilitation (DF) model of the glass transition. Utilizing a recently introduced measure of DF, we find that DF is important for particle motion in both the supercooled Dzugutov liquid and in the BKS silica melt, that mobility propagates continuously, and that this effect becomes increasingly pronounced with decreasing  $T$ . We show that, in both systems, dynamic facilitation is strongest on the time scale of the late- $\beta$  relaxation, where clusters of highly mobile neighboring particles escaping from their cages are largest and, except for the silicon atoms in BKS silica, stringlike motion is most prominent. By comparing the two systems, we show that the temperature dependence of one measure of DF as the mode-coupling temperature is approached from high temperature is similar, once the temperature dependence of the structural relaxation time in each system is scaled out.

## Introduction

The glass transition remains one of the longest-standing open problems in condensed matter physics.<sup>1,2</sup> Today, the phenomena that accompany the transition of a supercooled liquid to an amorphous solid are still vigorously investigated via experiments,<sup>3–13</sup> theory,<sup>14,15</sup> and computer simulations,<sup>16–23</sup> and much progress has been made. A relatively recent discovery that brings new insights to the dynamics of supercooled liquids is the notion of spatially heterogeneous dynamics (SHD),<sup>24–32</sup> where subsets of neighboring particles are found to be significantly more or less mobile over a given time interval, compared to the average particle, than would be expected from a Gaussian distribution of particle displacements. A Gaussian distribution is expected when relaxation processes are inertial or diffusive, as they are at very short and very long times in supercooled liquids. The cage-breaking process, which occurs at intermediate times, involves the dynamically correlated motion of neighboring particles. In many liquids, this correlated motion occurs along 1D, stringlike paths.<sup>10,18,33–38</sup> SHD, and to a slightly lesser extent stringlike motion, appears to be a ubiquitous feature of all glass-forming liquids. To date, SHD has been detected in atomistic<sup>18,33,34,37,42</sup> and polymeric liquids,<sup>16,36,39,40</sup> hard sphere systems,<sup>21,41</sup> and models of water<sup>35</sup> and silica.<sup>38</sup> It can thus be argued that any theory or model of a supercooled liquid that purports to completely describe the liquid dynamics approaching the glass transition must include SHD.

Recently, Garrahan and Chandler (GC) introduced a model<sup>43,44</sup> for the glass transition that centrally incorporates the concept

of SHD and that successfully describes key aspects of the transition of a liquid to a glass. Their model represents an important step forward in theoretical treatments of the glass transition because it provides an alternate view of the dynamical arrest that accompanies glass formation as compared with mode coupling and energy landscape theories and forces the close examination of the physical concepts underlying all of these theoretical approaches. At the heart of the GC model lies the concept of dynamic facilitation, meaning that mobile regions within the liquid enable neighboring regions to become mobile, a concept also central to earlier facilitation models<sup>45–47</sup> in which the GC model has its roots. In this way, GC argue, mobility propagates continuously and in a spatially correlated way throughout the liquid. They further argue that because particles in most regions of space are jammed at any given time mobility is made possible in only a relatively low fraction of spatial regions. GC therefore expect a clustering of mobile regions and thus a demixing of mobile and static regions. Such a demixing has been observed in simulations.<sup>18,39,48</sup> Thus, in the GC model, SHD arises naturally from limitations in particle mobility. Moreover, they argue that mobility propagation in fragile and strong liquids is manifested differently, leading to non-Arrhenius and Arrhenius  $T$  dependence, respectively, of the liquids' transport coefficients.

Here we examine some of the ideas put forth by GC, with a particular emphasis on dynamic facilitation and its relation to SHD. We test for DF in a molecular dynamics (MD) simulation of a supercooled monoatomic liquid modeled by the Dzugutov pair potential,<sup>49</sup> using a measure of DF recently introduced in a study of DF in MD simulations of the BKS model of silica.<sup>50</sup> That the dynamics are spatially heterogeneous and stringlike has already been firmly established for the Dzugutov system elsewhere.<sup>37,48,51,52</sup> Here we ascertain whether particle mobility propagates continuously through the system as GC suggests,<sup>44</sup> a necessary consequence of and thus evidence for dynamically facilitated particle motion. We compare our results with a recent

<sup>†</sup> Part of the special issue "David Chandler Festschrift".

\* To whom correspondence should be addressed. E-mail: sglotzer@umich.edu.

<sup>‡</sup> Department of Chemical Engineering.

<sup>§</sup> Department of Materials Science & Engineering.

<sup>||</sup> Current address: Institut für Physikalische Chemie, Westfälische Wilhelms-Universität Münster, Corrensstrasse 30, 48149 Münster, Germany. E-mail: mivogel@uni-muenster.de.

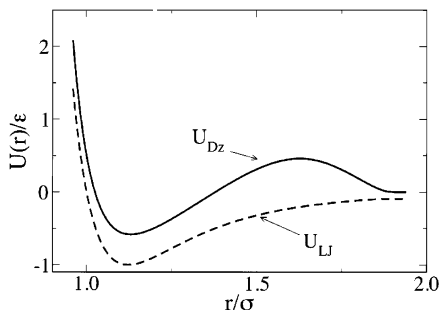


**Figure 1.** Dzugutov pair potential (—) plotted together with the Lennard-Jones potential (---). Note the second maximum in the Dzugutov potential, a feature that suppresses crystallization of the one-component supercooled liquid.

study of BKS silica<sup>50</sup> in order to establish similarities and differences in DF between these two systems of differing fragilities. Our investigations are performed at the level of individual particles, whereas the GC model is based on a coarse-grained description of dynamical behavior. Although the different level of description hampers a quantitative test of the GC model, it will nevertheless be shown that we can determine whether key assumptions of this model are justified.

### Model and Simulation Methodology

In the simulations presented here, we use the one-component Dzugutov interaction pair potential, which is known to favor icosahedral ordering in the first neighbor shell and was originally developed as a model of simple glass-forming liquid metals.<sup>49</sup> The Dzugutov potential is constructed to suppress crystallization common to most monoatomic systems by the introduction of a repulsive term representing the Coulomb interactions that are present in a liquid metal. This term gives rise to a second maximum that is strategically located to prevent particles residing in the second neighbor shell from finding energetically favorable sites as in an FCC or BCC configuration.<sup>53</sup> By introducing frustration locally in this way, crystallization into simple crystal structures is suppressed, and the system remains in the supercooled liquid state longer before crystallizing. In all, one attractive and two repulsive regimes characterize this potential, as shown in Figure 1, where the Dzugutov potential is plotted together with the Lennard-Jones (LJ) potential. The explicit form of the Dzugutov potential (eq 1) and the parameters of eq 1 are given below.

$$\begin{aligned}
 V &= V_1 + V_2 \\
 V_1 &= A(r^{-m} - B) \exp\left(\frac{c}{r-a}\right), r < a \\
 V_1 &= 0, r \geq a \\
 V_2 &= B \exp\left(\frac{d}{r-b}\right), r < b \\
 V_2 &= 0, r \geq b
 \end{aligned} \tag{1}$$

A	B	a	b	c	d	m
5.82	1.28	1.87	1.94	1.1	0.27	16

Dimensionless units are used in the simulation, where the energy has units of  $\epsilon$ , the temperature  $T$  has units of  $\epsilon/k_B$ , and  $k_B$  is the Boltzmann constant. Length has units of  $\sigma$ , and the dimensionless time  $t$  has units of  $\sigma^3/\epsilon$ .<sup>49</sup> The mass  $m$  and energy  $\epsilon$  are set to unity.

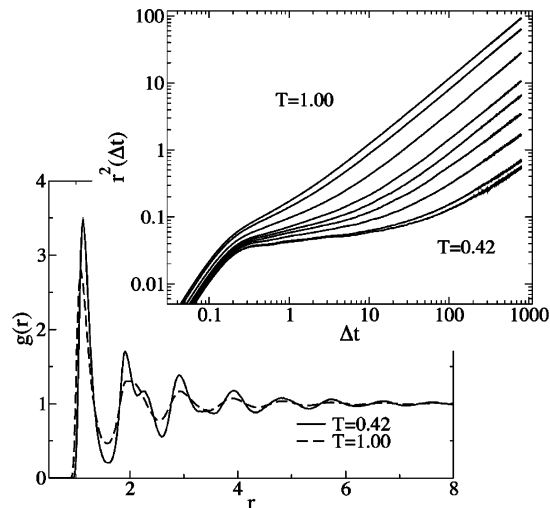


**Figure 2.** Mean squared displacement and pair correlation function calculated for the Dzugutov system at  $T = 1.00, 0.80, 0.65, 0.55, 0.52, 0.49, 0.46, 0.43,$  and  $0.42$ . Note that the plateau in the msd becomes more pronounced as  $T$  is lowered, indicating increased caging of particles over extended times. In addition, the  $g(r)$  curve for  $T = 0.42$  has a clearly split second peak, an indication of icosahedral ordering, which is substantially decreased at  $T = 1.00$ .

Our system contains  $N = 17\,576$  particles confined in a cubic box with a fixed density of 0.85. The range of temperatures studied is  $T = 1.0-0.42$ . The simulations are performed in the NVT (canonical) ensemble, and the temperature is maintained using a Berendsen thermostat.<sup>54</sup> The integration scheme used is velocity Verlet,<sup>55</sup> with a time step of  $0.01t$ . We start our simulation at  $T = 1.6$ , where we equilibrate the system for a sufficient time to remove any “memory” of the initial configuration. We then cool the system in a stepwise manner and equilibrate at each  $T$  before collecting data. At temperatures below  $T = 0.55$ , the liquid solidifies into a quasicrystal at times longer than those for which the data is presented here. The results presented in this study are obtained in the usual way by time averaging over a trajectory and, in addition, by averaging over several independent simulations for improved statistics. Through careful monitoring of our simulations, we have ensured that for the data presented here the system is quiescent and in metastable equilibrium. The data at the lowest  $T$  contains a small fraction of particles fixed in local icosahedral arrangements for the duration of the simulation,<sup>56</sup> but the system energy remains constant during the collection of data and no formation of a quasicrystalline phase is observed.

For reference, we show in Figure 2 plots of the mean squared displacement (msd),  $r^2(\Delta t)$ , and the pair correlation function  $g(r)$  for the Dzugutov liquid at various  $T$ , and these results are consistent with previous studies of the Dzugutov system.<sup>37</sup> The msd plot provides information on the average particle dynamics in the system, and the plateau in the msd becomes more pronounced with lower  $T$ , indicating the increased caging in the system with increased supercooling. The  $g(r)$  curve shown in Figure 2 for  $T = 0.42$  displays a distinct split of the second peak, denoting pronounced icosahedral ordering in the system.<sup>57</sup> At the highest  $T$  studied,  $T = 1.00$ , there is no split of the second peak in  $g(r)$ , but a broadening and a shoulder are starting to develop, indicating that some tendency for icosahedral particle arrangements is present in the system even at this high  $T$ .

We show in Figure 3 the self-part of the intermediate scattering function  $F_S(q, \Delta t)$  at the value of  $q$  corresponding to the first maximum in the static structure factor.<sup>37,49,52</sup> We see that a plateau develops in  $F_S(q, \Delta t)$  and becomes increasingly

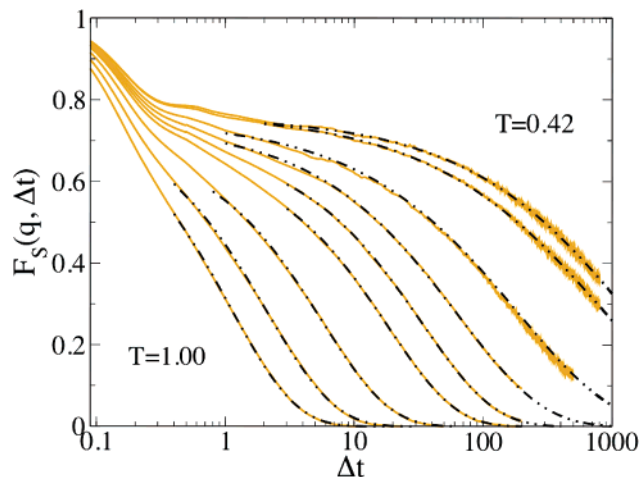


**Figure 3.** Self part of the intermediate scattering function for the Dzугutov system at the temperatures studied. A plateau develops as the temperature decreases, indicating a two-step relaxation process common to glass-forming liquids. The dashed–dotted lines show KWW fits to the long-time decay of  $F_S(q, \Delta t)$ . These fits are used to estimate the structural relaxation time  $\tau_{\text{self}}$  at each  $T$ .

pronounced as the simulation temperature is decreased, indicating the two-step relaxation process observed for supercooled liquids.<sup>58</sup> Also shown are Kohlrausch–Williams–Watts (KWW) fits of the long-time decay of  $F_S(q, \Delta t)$ . The form of the KWW fitting function used is  $A \exp[-(t/\tau)^\beta]$ , where  $A$ ,  $\tau$ , and  $\beta$  are the fitting parameters. The KWW fits (dashed–dotted lines) of the late-time decay in  $F_S(q, \Delta t)$  show good agreement with the data, and we use them to determine the relaxation time,  $\tau_{\text{self}} = (\tau/\beta) \Gamma[1/\beta]$ , at each  $T$ . Note that  $\beta$  is often referred to as a “stretching parameter” and is one indication of the degree of fragility of the liquid, where  $\beta = 1$  corresponds to a strong liquid and  $\beta$  decreases with increasing fragility.

## Results and Discussion

Our first examination of the dynamic facilitation model is to determine if mobility propagates continuously through the system. Although microscopic details are coarse-grained out in spin models of glass-forming liquids, predictions obtained from such models can still be compared with results generated using our particle-based model system. Hence, we analyze the positions of particles that are found to be highly mobile in back-to-back time intervals of equal length,  $\Delta t_{1 \rightarrow 2} = \Delta t_{2 \rightarrow 3} = \Delta t$ , as was done in a recent study of BKS silica.<sup>50</sup> Here we define “highly mobile” particles as the top 5% of the particles that moved the furthest over a given time interval. As was shown in several papers, this is a reasonable estimate of the fraction of particles that are escaping their cages at any given time.<sup>18,24,28,33,38</sup> We then calculate the probability distribution<sup>50</sup>  $P_F(r, \Delta t)$  of finding the minimum distance between mobile particles in  $\Delta t_{2 \rightarrow 3}$  that were nonmobile in  $\Delta t_{1 \rightarrow 2}$  and all mobile particles in  $\Delta t_{1 \rightarrow 2}$ . This distribution is then compared with the probability distribution  $P_F^*(r, \Delta t)$  obtained when particles used in the calculation are randomly selected from the nonmobile particles in  $\Delta t_{1 \rightarrow 2}$ . An example of the resulting distributions for  $T = 0.42$  and  $\Delta t = 80$  is shown in Figure 4, where the height of the first peak representing the dynamically facilitated particles (solid line) is clearly of greater magnitude than the height of the first peak of the distribution of the randomly chosen particles (dashed line). This means that there is indeed an increased probability that neighbors to mobile particles in  $\Delta t_{1 \rightarrow 2}$  become mobile themselves in  $\Delta t_{2 \rightarrow 3}$ , relative to a randomly chosen

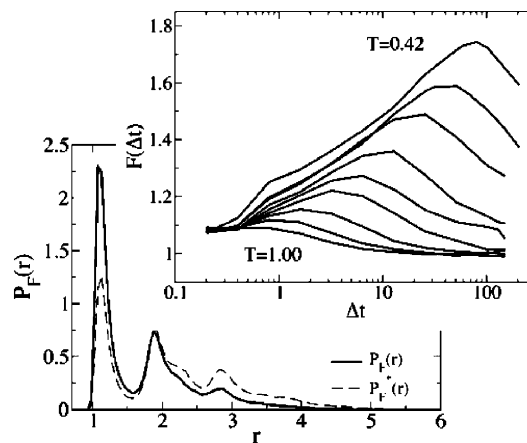


**Figure 4.** Probability distributions  $P_F(r, \Delta t)$  from  $T = 0.42$  and  $\Delta t = 80$ , where the solid curve representing the facilitated particles shows enhanced probability of finding small distances between particles that become mobile in  $\Delta t_{2 \rightarrow 3}$  and mobile particles in  $\Delta t_{1 \rightarrow 2}$  as compared to randomly chosen particles. The inset shows the strength of the dynamic facilitation at the studied temperatures.

particle. Hence, dynamic facilitation is present in the supercooled Dzугutov model system, and this effect is clearly detectable; the emergence of high particle mobility does not appear randomly within the liquid but it is facilitated by the presence of a neighboring mobile particle.

We next investigate the strength of the dynamic facilitation effect<sup>50</sup> by constructing the function  $F(\Delta t)$ , which is a ratio of the integral over the first peak in each of the probability distributions,

$$F(\Delta t) = \frac{\int_0^{r_{\min}} P_F(r, \Delta t) dr}{\int_0^{r_{\min}} P_F^*(r, \Delta t) dr} \quad (2)$$

where  $r_{\min}$  is the distance to the first minimum in  $g(r)$ ,  $r_{\min} = 1.6\sigma$ . The ratio given by  $F(\Delta t)$  is calculated for all  $T$  at different values of  $\Delta t$ , and the resulting curves are plotted in Figure 4.

The quantity  $F(\Delta t)$  constitutes a measure of the degree to which the probability that a neighbor of a mobile particle in  $\Delta t_{1 \rightarrow 2}$  becomes mobile in  $\Delta t_{2 \rightarrow 3}$  is enhanced relative to that of a random particle becoming mobile in  $\Delta t_{2 \rightarrow 3}$ . We see in Figure 4 that the effect of dynamic facilitation, as indicated by the peak height, increases with decreasing  $T$ . For example, at  $T = 0.42$  we find a maximum  $F(\Delta t) \approx 1.8$ , which means that there is an increased probability by a factor of about 1.8 that a particle neighboring a mobile particle in  $\Delta t_{1 \rightarrow 2}$  becomes mobile in  $\Delta t_{2 \rightarrow 3}$ , as compared to the random case. In other words, with respect to random statistics, the number of neighbors that achieve mobility nearly doubles.

We further see that the maximum effect of dynamic facilitation occurs at a time (for each  $T$ ) that corresponds to particles breaking out of their cages, as indicated by the end of the plateau in the mean squared displacement at the onset of diffusive particle motion. (See the msd plot in Figure 2 for reference.) Note that for the highest temperature investigated in this study,  $T = 1.0$ , the effect of dynamic facilitation is absent, and  $F(\Delta t)$  drops to a value of 1 at  $\Delta t \approx 1$ , a time corresponding to the onset of diffusive motion at that temperature. The trend we observe that the strength of dynamic facilitation increases with decreasing  $T$  and is absent at higher  $T$  is in agreement with predictions of the GC model.<sup>59</sup>

We find it noteworthy to compare the behavior of  $F(\Delta t)$  with the behavior of the average size (in terms of mass or number

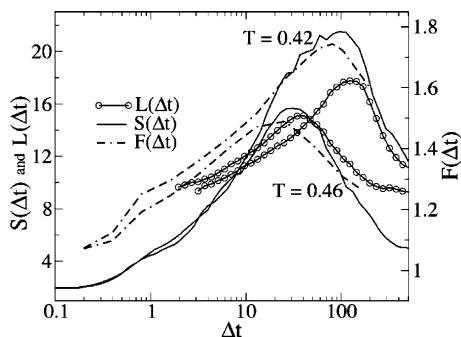


**Figure 5.** Examples of how the average string length  $L(\Delta t)$ , the average cluster size  $S(\Delta t)$ , and the effect of dynamic facilitation  $F(\Delta t)$  initially increase, achieve maxima, and then decrease over a given time interval,  $\Delta t$ , for two values of  $T$ . Note that the  $L(\Delta t)$  data is multiplied by a factor of 3 to aid visualization.

of particles) of mobile particle clusters,  $S(\Delta t)$ , and the average string lengths (again in terms of the number of particles),  $L(\Delta t)$ , that were thoroughly investigated in previous SHD studies<sup>37,48</sup> using this model system. Examples of the behavior of these quantities are shown in Figure 5, where the  $S(\Delta t)$  and  $L(\Delta t)$  data are taken from Gebremichael et al.<sup>37</sup> and the  $L(\Delta t)$  data is multiplied by a factor of 3 to aid visualization. By monitoring particle movement over a *single* time interval, it was found in these previous studies that highly mobile particles move cooperatively to form short 1D strings, suggesting that the motion of a particle enables the motion of particles in the first neighbor shell. However, it was not established quantitatively whether this form of mobility continuously propagates through the system because such information is not contained in a two-time (i.e., single time interval) quantity such as  $S(\Delta t)$  or  $L(\Delta t)$ . Instead, quantification of the tendency for continuous propagation of motion may be extracted via a three-time correlation function such as  $F(\Delta t)$  that monitors particle movement over *two* contiguous time intervals. An examination of Figure 5 shows that  $F(\Delta t)$  grows, reaches a maximum, and then decreases as  $\Delta t$  is increased. This means that particle mobility is facilitated and that this facilitation has a time window over which it is most pronounced. Thus, the behavior of  $F(\Delta t)$  provides new information and is evidence that the observed correlated mobility indeed propagates *continuously* through the system, in agreement with the GC model.<sup>44</sup>

From Figure 5, we also see that the magnitudes of the different quantities are magnified as  $T$  is lowered. This is true for the complete range of temperatures that we investigate, though we show data only from  $T = 0.42$  and  $0.46$  here. This observation is also in agreement with a recent study using the GC model.<sup>59</sup>

Furthermore, we find that the times at which the effect of dynamic facilitation is at a maximum for all  $T$ s correspond well with the times that  $S(\Delta t)$  and  $L(\Delta t)$  also have been found to be at their maximum for this system.<sup>37</sup> We find that there is a consistent trend for  $T < T = 0.65$  where the effect of dynamic facilitation is clear. The time  $t_F$  where the maximum effect in  $F(\Delta t)$  is found to occur, the time  $t_S$  of the maximum in  $S(\Delta t)$ , and the time  $t_L$  at which the maximum in  $L(\Delta t)$  is detected all increase with decreasing  $T$ . These trends are depicted in Figure 6, where the  $t_L$  and  $t_S$  data are taken from Gebremichael et al.<sup>37</sup> Thus, in this system the measure  $F(\Delta t)$  of dynamic facilitation reaches a maximum (we label these values  $F(\Delta t)_{\text{MAX}}$ ) at approximately the same time that a maximum in the spatial heterogeneity of the particle dynamics as measured by correlations in high particle mobility based on neighborhood, and a maximum in cooperativity, is observed. In addition, these events

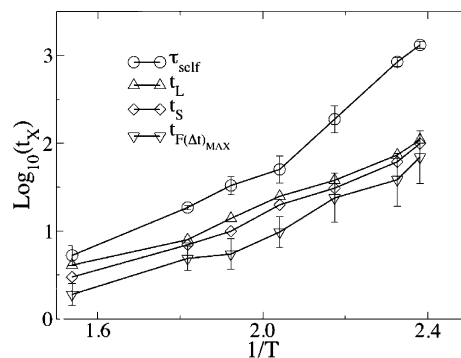


**Figure 6.** Time constants plotted versus  $1/T$  for the Dzугutov liquid. As  $T$  is lowered, the structural relaxation time  $\tau_{\text{self}}$  increases more rapidly than the characteristic times at which the maximum average string length, maximum average mobile-particle cluster size, and maximum effect of DF are observed.

all occur on a time scale that is substantially smaller than the structural relaxation time of the self-intermediate scattering function (i.e.,  $\tau_{\text{self}} \gg t_L \geq t_S \geq t_F$ ) within statistical error. We further find that  $\tau_{\text{self}}$  increases more rapidly on cooling relative to the other time constants. Because of the limited temperature range and the nonnegligible error bars in the data, we cannot clearly distinguish, at this point, whether  $t_F$  for the Dzугutov liquid shows non-Arrhenius behavior like the  $\alpha$  and  $\beta$  relaxation times or Arrhenius behavior, as is expected for the rate of creation of excitations in facilitated models. Future studies on different liquids that can be cooled below  $T_{\text{MCT}}$  without crystallization may help to answer this question.

The results shown in Figure 6 agree well with the findings for BKS silica,<sup>50</sup> where  $\tau_{\text{self}} \gg t_S \approx t_F$  was also observed both in the fragile regime where the transport coefficients have a non-Arrhenius  $T$  dependence as well as in the  $T$  range where the transport coefficients become Arrhenius, corresponding to a fragile-to-strong crossover in the liquid. Hence, this relationship appears to be independent of fragility. However, the decoupling of  $\tau_{\text{self}}$  from  $t_F$  and so forth with decreasing  $T$  is more pronounced for the Dzугutov liquid than for BKS silica.<sup>60</sup>

We now compare the behavior of  $F(\Delta t)$  in the Dzугutov liquid with its behavior in the BKS silica system.<sup>50</sup> The Dzугutov liquid is known to be a fragile glass former with a  $\beta$  value<sup>37</sup> of 0.5, whereas the oxygen ( $\beta = 0.83$ ) and silicon ( $\beta = 0.85$ ) atoms in BKS silica<sup>38</sup> show  $\beta$  values of a much stronger glass-forming liquid. Therefore, we are in a position to study the effects of fragility on the relevance of mobility propagation.

Because different temperature scales are used in the simulations of the two systems, we use a normalized temperature scale for which the results can be directly compared. For the results shown here, we use the critical  $T$  of MCT,<sup>14</sup>  $T_{\text{MCT}}$ , as a characteristic parameter for the normalization; however, we determined that the observed trends are independent of the temperature used for normalization by using a  $T \approx T_0$  close to the onset of dynamical heterogeneities for both systems (not shown). The values of  $T_{\text{MCT}}$  used here are obtained from the literature and are 3330 K for BKS silica<sup>61</sup> and 0.4 (in reduced units) for the Dzугutov liquid.<sup>37,52</sup> In Figure 7, we show the results obtained when plotting  $F(\Delta t)_{\text{MAX}}$  versus the reduced temperature  $(T - T_{\text{MCT}})/T_{\text{MCT}}$ . Included in the Figure are data obtained from the Dzугutov liquid and from the silicon atoms and oxygen atoms, respectively, in the BKS system.

From Figure 7, we see that at comparable values of the reduced temperature the trends in  $F(\Delta t)_{\text{MAX}}$  are similar for the two systems, within statistical error. This demonstrates that

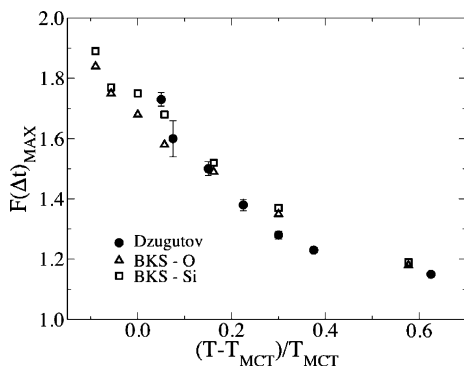


**Figure 7.** Maximum values,  $F(\Delta t)_{\text{MAX}}$ , reflecting the maximum strength of dynamic facilitation at each temperature plotted versus a temperature scale normalized by  $T_{\text{MCT}}$  for the two systems. The temperature dependence of DF appears to be similar for the two systems above  $T_{\text{MCT}}$ . Near  $T_{\text{MCT}}$ , however, we cannot rule out that the values of  $F(\Delta t)_{\text{MAX}}$  for the Dzugutov liquid may begin to increase more rapidly with decreasing  $T$  without additional data at lower  $T$ , which is unattainable because of crystallization of the liquid. The error bars for the Dzugutov data represent statistical errors in the sampling. Several independent runs, each containing a minimum of 350 time averages, are carried out at each value of  $T$ . At each  $T$ , the distribution of values of  $F(\Delta t)_{\text{MAX}}$  are Gaussian, and the width of the distribution varies from very narrow at  $T > 0.5$  to very broad at  $T = 0.43$  (where 1750 time averages for each run are performed). The error bars directly reflect the width of this distribution. At  $T = 0.42$ , the small error bar reflects the small width of the distribution of values of  $F(\Delta t)_{\text{MAX}}$ , suggesting insufficient statistics at this low  $T$  (again due to the tendency of the liquid to crystallize at low  $T$ ).

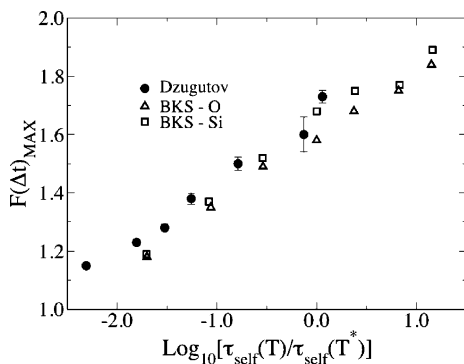


**Figure 8.** Maximum values,  $F(\Delta t)_{\text{MAX}}$ , in Figure 7 plotted versus a normalized relaxation time. Similar trends for the different systems are again observed above  $T_{\text{MCT}}$ .

mobility propagates continuously in both of these glass-forming liquids, despite the difference in fragility, which is in agreement with the GC model. To investigate further the role of fragility, we scale out the temperature dependence of  $\tau_{\text{self}}$  and plot  $F(\Delta t)_{\text{MAX}}$  versus the log of a normalized relaxation time. The normalization is necessary because of the different time units used in the Dzugutov and the BKS simulations. The normalization is obtained by dividing  $\tau_{\text{self}}$  at each  $T$  by  $\tau_{\text{self}}(T^*)$ , where we choose  $T^* \equiv (T - T_{\text{MCT}})/T_{\text{MCT}} = 0.057$ . This value of  $T^*$  is chosen because data points exist at this reduced temperature for both systems. The results are shown in Figure 8. We see that  $F(\Delta t)_{\text{MAX}}$  plotted versus the scaled relaxation time  $\tau_{\text{self}}/\tau_{\text{self}}(T^*)$  increases in a manner similar to that found in Figure 7 for both systems.

These results imply that DF is of similar importance in both liquids in this (relatively high) temperature range, and the extent to which particle motion is facilitated at a given temperature depends only on the structural relaxation time at that temperature, once fragility is scaled out. We suggest that the universal-

ity of these findings should be checked in other fragile glass-forming liquids, such as BLJ, where data at and below  $T_{\text{MCT}}$  is available.

## Summary

We find that dynamic facilitation is important for particle motion in the supercooled Dzugutov liquid and that mobility tends to propagate continuously through the system as the GC model predicts. We also find that the effect of DF becomes increasingly pronounced with decreasing  $T$  and that DF is of minimal importance for particle movement at high  $T$ , as was recently shown<sup>59</sup> in another system using the GC model. Combining our results with those obtained for BKS silica,<sup>50</sup> we show that DF is evident in both fragile and strong liquids, with a similar  $T$  dependence, at least in terms of the particular quantity  $F(\Delta t)$  calculated here, at temperatures below the onset of SHD but above the mode-coupling temperature. Because  $F(\Delta t)$  is constructed solely to measure the extent to which mobility propagates continuously, as GC suggests, no information on measures such as the persistence length of mobility propagation or the creation of excitations needed for mobility to occur can be commented on in this work; instead, the measurement of such quantities is left for future work.

**Acknowledgment.** We thank D. Chandler, J. Garrahan, Y. Gebremichael, A.S. Keys, and P.H. Poole for stimulating discussions. M.V acknowledges funding of the DFG through the Emmy Noether-Programm. M.N.J.B. acknowledges funding from the GAANN Fellowship Program and the NASA Office of Biological and Physical Research under grant NNCO4GA43G.

## References and Notes

- (1) Ediger, M. D. *J. Phys. Chem.* **1996**, *100*, 13200.
- (2) Sillescu, H. *J. Non-Cryst. Solids* **1999**, *243*, 81.
- (3) Bartsch, E.; Frenz, V.; Sillescu, H. *J. Non-Cryst. Solids* **1994**, *172*, 88.
- (4) Cicerone, M. T.; Blackburn, F. R.; Ediger, M. D. *J. Chem. Phys.* **1995**, *102*, 471.
- (5) Cicerone, M. T.; Blackburn, F. R.; Ediger, M. D. *Macromolecules* **1995**, *28*, 8224.
- (6) Cicerone, M. T.; Ediger, M. D. *J. Chem. Phys.* **1995**, *103*, 5684.
- (7) Sillescu, H. *J. Chem. Phys.* **1996**, *104*, 4877.
- (8) Sillescu, H. *Phys. Rev. E* **1996**, *53*, 2992.
- (9) Tracht, U.; Wilhelm, M.; Heuer, A.; Feng, H.; Schmidt-Rohr, K.; Spiess, H. W. *Phys. Rev. Lett.* **1998**, *81*, 2727.
- (10) Weeks, E. R.; Crocker, J. C.; Levitt, A. C.; Schofield, A.; Weitz, D. A. *Science* **2000**, *287*, 627.
- (11) Russell, E. V.; Israeloff, N. E. *Nature* **2000**, *408*, 695.
- (12) Reinsberg, S. A.; Qiu, X. H.; Wilhelm, M.; Spiess, H. W.; Ediger, M. D. *J. Chem. Phys.* **2001**, *114*, 7299.
- (13) Deschenes, L. A.; Vanden Bout, D. A. *Science* **2001**, *292*, 255.
- (14) Gotze, W.; Sjogren, L. *Rep. Prog. Phys.* **1992**, *55*, 241.
- (15) Adam, G.; Gibbs, J. H. *J. Chem. Phys.* **1965**, *43*, 139.
- (16) Bennemann, C.; Paul, W.; Binder, K.; Dunweg, B. *Phys. Rev. E* **1998**, *57*, 843.
- (17) Kob, W. *J. Phys.: Condens. Matter* **1999**, *11*, R85.
- (18) Donati, C.; Glotzer, S. C.; Poole, P. H.; Kob, W.; Plimpton, S. J. *Phys. Rev. E* **1999**, *60*, 3107.
- (19) Rosche, M.; Winkler, R. G.; Reineker, P.; Schulz, M. *J. Chem. Phys.* **2000**, *112*, 3051.
- (20) Binder, K. *J. Non-Cryst. Solids* **2000**, *274*, 332.
- (21) Doliwa, B.; Heuer, A. *Phys. Rev. E* **2000**, *61*, 6898.
- (22) Binder, K. *J. Non-Cryst. Solids* **2002**, *307*, 1.
- (23) Binder, K.; Baschnagel, J.; Paul, W. *Prog. Polym. Sci.* **2003**, *28*, 115.
- (24) Kob, W.; Donati, C.; Plimpton, S. J.; Poole, P. H.; Glotzer, S. C. *Phys. Rev. Lett.* **1997**, *79*, 2827.
- (25) Heuer, A.; Okun, K. *J. Chem. Phys.* **1997**, *106*, 6176.
- (26) Poole, P. H.; Donati, C.; Glotzer, S. C. *Physica A* **1998**, *261*, 51.
- (27) Bennemann, C.; Donati, C.; Baschnagel, J.; Glotzer, S. C. *Nature* **1999**, *399*, 246.
- (28) Glotzer, S. C.; Donati, C. *J. Phys.: Condens. Matter* **1999**, *11*, A285.

- (29) Glotzer, S. C.; Novikov, V. N.; Schroder, T. B. *J. Chem. Phys.* **2000**, *112*, 509.
- (30) Glotzer, S. C.; Gebremichael, Y.; Lacevic, N.; Schroder, T. B.; Starr, F. W. Spatially Heterogeneous Dynamics in Liquids near Their Glass Transition. In *Liquid Dynamics: Experiment, Simulation, and Theory*; Fourkas, J. T., Ed.; American Chemical Society: Washington, DC, 2002; Vol. 820, p 214.
- (31) Glotzer, S. C.; Gebremichael, Y.; Lacevic, N.; Schroder, T. B.; Starr, F. W. *Comput. Phys. Commun.* **2002**, *146*, 24.
- (32) Richert, R. *J. Phys.: Condens. Matter* **2002**, *14*, R703.
- (33) Donati, C.; Douglas, J. F.; Kob, W.; Plimpton, S. J.; Poole, P. H.; Glotzer, S. C. *Phys. Rev. Lett.* **1998**, *80*, 2338.
- (34) Schroder, T. B.; Sastry, S.; Dyre, J. C.; Glotzer, S. C. *J. Chem. Phys.* **2000**, *112*, 9834.
- (35) Giovambattista, N.; Starr, F. W.; Sciortino, F.; Buldyrev, S. V.; Stanley, H. E. *Phys. Rev. E* **2002**, *65*, 041502.
- (36) Aichele, M.; Gebremichael, Y.; Starr, F. W.; Baschnagel, J.; Glotzer, S. C. *J. Chem. Phys.* **2003**, *119*, 5290.
- (37) Gebremichael, Y.; Vogel, M.; Glotzer, S. C. *J. Chem. Phys.* **2004**, *120*, 4415.
- (38) Vogel, M.; Glotzer, S. C. *Phys. Rev. E* **2004**, *70*, 061504.
- (39) Gebremichael, Y.; Schroder, T. B.; Starr, F. W.; Glotzer, S. C. *Phys. Rev. E* **2001**, *64*, 051503.
- (40) Glotzer, S. C.; Paul, W. *Annu. Rev. Mater. Res.* **2002**, *32*, 401.
- (41) Doliwa, B.; Heuer, A. *J. Phys.: Condens. Matter* **1999**, *11*, A277.
- (42) Vogel, M.; Doliwa, B.; Heuer, A.; Glotzer, S. C. *J. Chem. Phys.* **2004**, *120*, 4404.
- (43) Garrahan, J. P.; Chandler, D. *Phys. Rev. Lett.* **2002**, *89*, 035704.
- (44) Garrahan, J. P.; Chandler, D. *Proc. Natl. Acad. Sci. U.S.A.* **2003**, *100*, 9710.
- (45) Glarum, S. H. *J. Chem. Phys.* **1960**, *33*, 639.
- (46) Phillips, M. C.; Barlow, A. J.; Lamb, J. *Proc. R. Soc. London, Ser. A* **1972**, *329*, 193.
- (47) Fredrickson, G. H.; Andersen, H. C. *Phys. Rev. Lett.* **1984**, *53*, 1244.
- (48) Gebremichael, Y.; Vogel, M.; Glotzer, S. C. *Mol. Simul.* **2004**, *30*, 281.
- (49) Dzugutov, M. *Phys. Rev. A* **1992**, *46*, R2984.
- (50) Vogel, M.; Glotzer, S. C. *Phys. Rev. Lett.* **2004**, *92*, 255901.
- (51) Dzugutov, M.; Simdyankin, S. I.; Zetterling, F. H. M. *Phys. Rev. Lett.* **2002**, *89*, 195701.
- (52) Zetterling, F. H. M.; Dzugutov, M.; Simdyankin, S. I. *J. Non-Cryst. Solids* **2001**, *293*, 39.
- (53) Roth, J.; Denton, A. R. *Phys. Rev. E* **2000**, *61*, 6845.
- (54) Berendsen, H. J. C.; Postma, J. P. M.; Vangunsteren, W. F.; Dinola, A.; Haak, J. R. *J. Chem. Phys.* **1984**, *81*, 3684.
- (55) Allen, M. P.; Tildesley, D. J. *Computer Simulation of Liquids*; Oxford University Press: New York, 1987.
- (56) Keys, A.; Glotzer, S. C. Unpublished results, 2004.
- (57) Nelson, D. R. *Phys. Rev. B* **1983**, *28*, 5515.
- (58) Kob, W.; Andersen, H. C. *Phys. Rev. Lett.* **1994**, *73*, 1376.
- (59) Berthier, L.; Garrahan, J. P. *Phys. Rev. E* **2003**, *68*, 041201.
- (60) Vogel, M.; Glotzer, S. C. Unpublished results, 2004.
- (61) Horbach, J.; Kob, W. *Phys. Rev. B* **1999**, *60*, 3169.